

## DEVELOPMENT OF NOVEL DIGLYCIDYL AND TETRAGLYCIDYL PHOSPHORUS MODIFIED EPOXY RESINS FOR HIGH PERFORMANCE AEROSPACE APPLICATIONS

**K. Shree Meenakshi**  
Anna University  
INDIA  
shreemeenakshik@gmail.com

**S. Ananda Kumar**  
Anna University  
INDIA  
sreeanand@gmail.com

### ABSTRACT

This research work focuses on a comparative study between phosphorus containing diglycidyl and tetraglycidyl epoxy resins to find the best between them for use in high performance aerospace applications. The synthesis of 9, 10-dihydro-9-oxa-10-phosphaphenanthrene-10-oxide modified diglycidyl epoxy (DOPO-epoxy) and phosphorus containing tetraglycidyl epoxy was carried out and their structures were characterized by spectral analysis. Nanoclay (Nanomer 1.30E) and nano-reinforcement (POSS-amine) were incorporated into the epoxy resins to study their influence on different properties. Curing of both the epoxy resins was done with diaminodiphenyl methane (DDM). Mechanical, thermal, flame retardant and water absorption behaviour of the two tetra epoxy resins were compared with each other and the interesting results thus obtained are discussed.

**Keywords:** Epoxy resins, Fourier transformed infrared spectroscopy (FTIR), Thermo gravimetric analysis (TGA), mechanical properties and flame retardancy.

### INTRODUCTION

Epoxy resins are widely used in many applications due to their low cost, ease of processing, low shrinkage, good chemical and electrical resistance and mechanical properties [1–5]. However, their application is restricted for use at high temperature as they degrade easily to lose their mechanical and physical properties. Another important property that needs to be improved for epoxy resin is its inadequate flame retardancy that prevents its use in electronic applications. Halogen-containing compounds are commonly used as flame-retardants in epoxy resins, either by blending or chemical modification to improve their thermal and flame-retardant behavior. However, this type of modification is limited due to toxic gas emissions [6-8]. Various fillers such as antimony trioxide, magnesium hydroxide, and boron based compounds are also often used with epoxy resins to improve their flame resistance, which results in a release of toxic and corrosive fumes during thermal decomposition and making their further usage limited.

### LITERATURE REVIEW

Recently, organo-phosphorus compounds have been used as effective fire retardants, usually as additives and more recently by being incorporated into the backbone of the epoxy resin [6], epoxy resin diglycidylether of bisphenol-A (DGEBA) has been modified with diphenylphosphonic chloride and polymerized the system with diethyltrianmine (DETA) [7]. More recently, researchers have developed siloxane modified DGEBA with bis (3-aminophenyl) phenylphosphine oxide (BMIPO) to produce silicon/phosphorous-containing epoxy flame retardant polymer [8]. Scientists also synthesized phosphorous-containing bi-functional DGEBA-type epoxy and showed that its thermal properties can be improved to

greater extent [9]. Furthermore, the flame retardancy and thermal stability of the epoxy resins can be improved by the simultaneous incorporation of a phosphorous group along with nano clay and nano-reinforcements to the backbone of epoxy resin [10].

Clay-containing polymeric nanocomposite (CPNC) has several advantages over the matrix polymer or classical composites. The major improvements are in: modulus, impact strength, heat resistance, dimensional stability, barrier properties, flame retardancy, optical properties, ionic conductivity, and thermal stability [11]. Through the addition of nanoclay, the plane strain fracture toughness of epoxy matrix can be dramatically enhanced [12].

On the other hand, polyhedral oligomeric silsesquioxanes (POSS) are new generation nano reinforcing materials that can be used as flame-retardants in thermosetting resins [13, 14]. These materials are chemically modified particles of silica, have dimensions at the nanometer scale. Their inorganic (silicon based) structure provides thermal stability and fire resistance, whereas their organic (carbon based) structure provides compatibility and/or reactivity with the resins [15]. This covalent bonding allows the POSS to react into the thermoset network and reinforce the polymer on the molecular level. These chains act as nanoscale reinforcement that provides exceptional gains in heat resistance [15,16]. POSS has been used as an additive in heat resistant paints and coatings, mechanical property modifiers, cross-linking agents, and viscosity modifiers [13]. Because POSS exists on the nanoscale, the motions of the chain can be controlled and the processing and moldability of the resin is theoretically maintained. POSS can be easily incorporated into common plastics via copolymerization or blending and hence requires little or no alteration to existing manufacturing processes. In addition, POSS molecules are odorless, release no volatile organic compounds, and are therefore environmentally friendly even when ignited.

Hence an attempt has been made in the present study to develop diglycidyl and tetraglycidyl epoxy resins by modifying them with reactive phosphorous compounds with an incorporation of organic modified clay (Nanomer 1.30E) and nano reinforcement. The effect of nano clay and nano reinforcements on the thermal and flame retardant properties of modified epoxy resins is studied. The resulting materials were characterized by spectral techniques and their mechanical, thermal and flame retardancy was evaluated by standard testing methods. Comparative studies of the properties of these resins are done. The results thus obtained from this study are discussed.

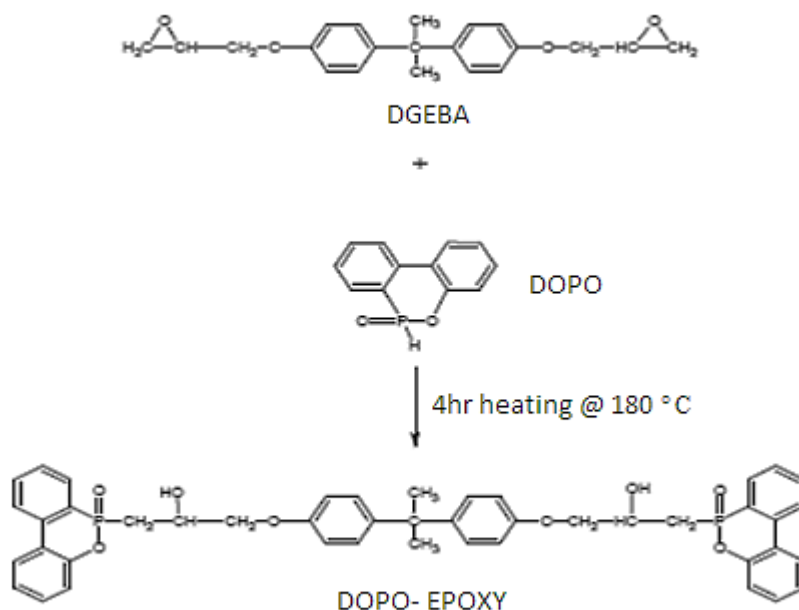
## METHODOLOGY

### Materials

All chemicals are reagent grade and were used without further purification. DGEBA (GY 250) and 4, 4'-diaminodiphenylmethane (DDM) were obtained from Huntsman, USA. Epichlorohydrin and sodium hydroxide was obtained from s-d fine chemical company, India. Triphenyl phosphine oxide was obtained from Alfa-Aaser, Germany. 9, 10-dihydro-9-oxa-10-phosphaphenanthrene-10-oxide (DOPO) was obtained from ADD, ABT, Netherlands. 1,3,5,7,9,11,14 Hepta siloxane-endo-3, 7,14 triol was obtained from Sigma Aldrich. Nano clay was obtained from Nanocor, USA Aminopropyltrimethoxysilane ( $\gamma$ -APS), stannous chloride and sulphuric acid were obtained from Merck (Germany). THF (Tetrahydrofuran) and benzene was obtained from Sisco research laboratories, India. Hydrochloric acid was obtained from Hi-pure, India.

**Synthesis of phosphorus containing diglycidyl epoxy resin**

DGEBA epoxy resin (250 g) was charged into a three-neck round-bottom flask and heated to 130°C in an oil bath connected to a temperature controller. DOPO (66g) was added and mixed by a mechanical stirrer at 500 rpm, maintaining the temperature at 130°C until a clear solution was obtained (Scheme 1). The temperature was then raised to 180°C and stirring continued for a further 5hr until a transparent solution of 3% phosphorus-DGEBA epoxy was obtained.

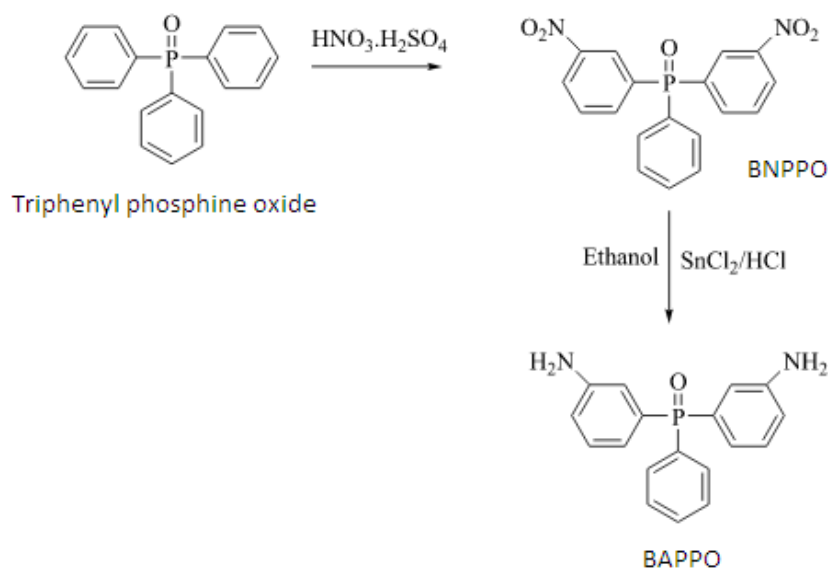


Scheme 1: Synthesis of phosphorus containing diglycidyl epoxy resin

**Synthesis of phosphorus containing tetraglycidyl epoxy resin****Synthesis of bis (3-aminophenyl) phenyl phosphine oxide (BAPPO)**

Triphenyl phosphine oxide (27.8 g) was placed in a 500 ml round bottom flask equipped with stirrer and nitrogen atmosphere and 200 ml of 96% sulphuric acid was added to it. The reactant was dissolved and the reaction system was cooled to -5°C with an ice/salt bath. A solution of 14.5 g of fuming nitric acid in 100ml of sulphuric acid was added drop wise over a period of 2hrs. The reaction system was kept at room temperature for another 8hrs. The reaction mixture was hydrolyzed by 2 litre of ice and the mixture was extracted with chloroform and washed with an aqueous sodium bicarbonate solution until neutral pH. The solvent was removed. The solid residue was recrystallised from absolute ethanol to get bis (3-nitrophenol) phenyl phosphine oxide (BNPPO). BNPPO was taken in a 1000 ml round bottom flask with 180 g of anhydrous powdered tin (II) chloride. A solution of 200 ml fuming hydrochloric acid in 400 ml ethanol was introduced in to the flask. The reaction mixture was stirred at room temperature for 5hr. the solution was concentrated and then neutralized by 25% of aqueous NaOH solution. The obtained solution was extracted with chloroform. The organic layer was collected and concentrated under a reduced pressure. The

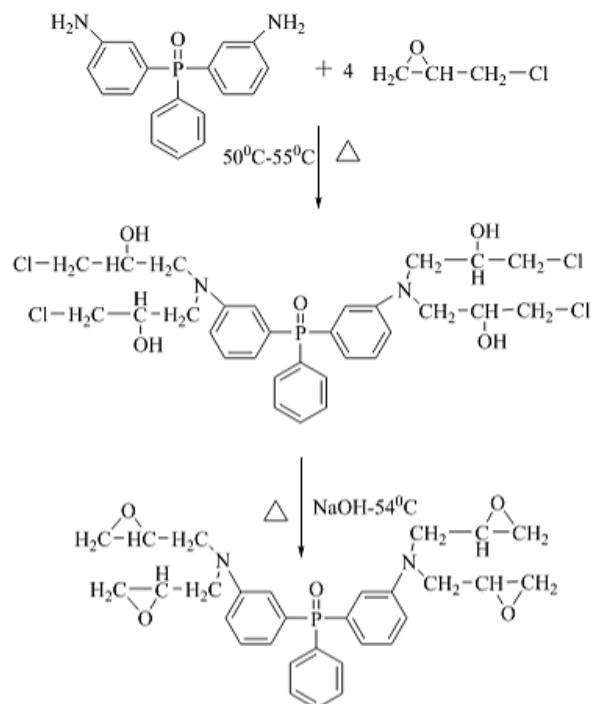
obtained solid was recrystallized from dichloromethane to give a pure product of BAPPO (Scheme 2).



Scheme 2: Synthesis of bis (3-aminophenyl) phenyl phosphine oxide (BAPPO)

#### Synthesis of phosphorus containing tetra functional epoxy

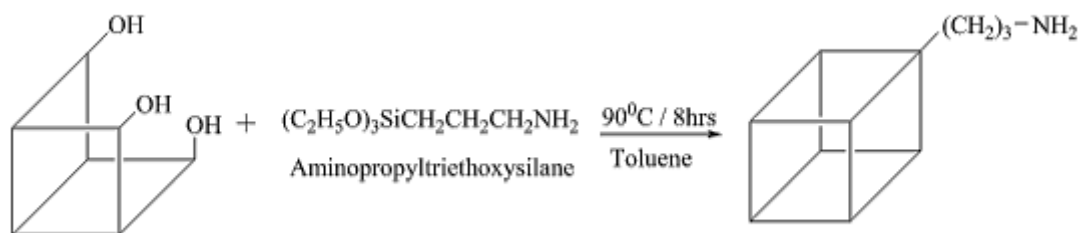
Epichlorohydrin (576.3g) was taken in a 1 liter three necked round bottom flask provided with a mechanical stirrer, nitrogen inlet tube and a water condenser. This was heated to  $50^\circ\text{C}$  in a water bath. Then 93.8g of Bis (3-aminophenyl) phenyl phosphine oxide was stirred continuously for 4hrs at the temperature range of  $50\text{--}55^\circ\text{C}$  under the nitrogen atmosphere. Chlorohydrin, the intermediate product was formed and the excess epichlorohydrin used was distilled off under vacuum. Then 113.7g of 40% NaOH solution was added dropwise for 1hr at  $54^\circ\text{C}$ . Then the reaction was continued at this temperature for another 1hr. Then 250ml benzene was added to the mixture and stirred for 15min to get two layers. The aqueous layer with NaCl by-product was formed. The organic layer was purified by washing several times with water. Then benzene was evaporated to get light brown coloured liquid epoxy product (Scheme 3).



Scheme 3: Synthesis of phosphorus containing tetra functional epoxy

### Synthesis of amine functionalized POSS (POSS -NH<sub>2</sub>)

The synthesis of POSS-NH<sub>2</sub> was carried out as per the reported procedure. Stoichiometric amount of POSS-triol (11.84g) dissolved in dry toluene was mixed with aminopropyltriethoxysilane (1.63g) in a 50ml round bottomed flask and refluxed for 8 hours at 90°C. Then filtrate is then subjected to solvent evaporation to obtain the desired product (Scheme 4).



Scheme.4: Synthesis of amine functionalized POSS

### Fabrication of Neat Resin Laminates

In order to study the properties of the novel epoxy resins, neat resin laminates were prepared by reacting synthesized epoxies with nanoclay, nanoreinforcement (POSS) and curing agent (DDM) in stoichiometric quantities as shown in Table 1.

**Table 1.** Fabrication of Neat Resin Laminates

NAME OF THE SYSTEM	EPOXY RESIN USED	% of NANO CLAY	% of POSS-AMINE
E	Phosphorus difunctional epoxy resins (DOPO epoxy)	-	-
F	Phosphorus difunctional epoxy resins (DOPO epoxy)	2.5	-
G	Phosphorus difunctional epoxy resins (DOPO epoxy)	5.0	-
H	Phosphorus difunctional epoxy resins (DOPO epoxy)	-	2.5
I	Phosphorus tetrafunctional epoxy resins	-	-
J	Phosphorus tetrafunctional epoxy resins	2.5	-
K	Phosphorus tetrafunctional epoxy resins	5.0	-
L	Phosphorus tetrafunctional epoxy resins	-	2.5

For the fabrication of nanocomposite, the Nanoclay (Nanomer 1.30E) was dried for 24 hour at 50°C under vacuum. The layered silicate was dispersed in the resin at 80°C using sonicator/stirrer at 500 rpm. After mixing the resin/clay for 1hr, the curing agent was added to it. The curing temperature and curing time of the epoxy resins are given below in Table 2.

**Table 2.** Curing temperatures of the various epoxy systems

Name of the System	Curing temperature	
	PRECURE	POSTCURE
E	120°C. 6hr	200°C. 2hr
F	120°C. 6hr	200°C. 2hr
G	120°C. 6hr	200°C. 2hr
H	120°C. 6hr	200°C. 2hr
I	120°C. 3hr	180°C. 2hr
J	100°C. 2hr, 120°C. 2hr	175°C. 4hr
K	100°C. 2hr, 120°C. 2hr	175°C. 4hr
L	100°C. 2hr, 120°C. 2hr	175°C. 4hr

### Characterization

**Infrared (IR)/Fourier transform infrared (FTIR) spectra:** The IR spectra were recorded on a Perkin-Elmer 781 infrared spectrometer using KBr pellets for solid sample. NaCl was used for taking IR spectra of viscous liquid samples.

**Nuclear Magnetic Resonance spectroscopy (NMR):** <sup>1</sup>H NMR spectra were run on a bruker 400 MHz spectrometer using CDCl<sub>3</sub> and DMSO as solvents and tetramethylsilane as internal standard proton decouple.

**Thermal analysis:** Thermo gravimetric analysis of the polymeric matrices was carried out in TGA-Thermal Analyst Perkin Elmer (TA instrument USA) at a heating of 10°C per minute in an inert atmosphere to determine thermal degradation temperature and percentage weight loss.

**Differential scanning calorimetry:** Differential scanning calorimeter NETZSCH DSC 200PC (TA instrument USA) was used to determine the glass transition temperature of the polymer matrices with a heating rate of 10°C / minute.

### Mechanical characteristics

Mechanical properties such as tensile strength, tensile modulus, flexural strength, flexural modulus and impact strength of matrix were studied as per ASTM standards.

**Tensile properties:** Tensile strength is a measurement of the ability of a material to withstand forces that tend to pull it apart and to determine to what extent the material stretches before breaking. Tensile modulus is an indication of the relative stiffness of a material, which can be determined from a stress–strain diagram. Tensile properties were studied as per as ASTM- D3039 using universal testing machine model (HTE–Series–H50K–S model, Hounsfield test equipments Ltd. UK) at 2mm/min cross head speed, using specimen with a width of 25 mm, length of 200 mm and thickness of 3 mm. A distance of 115 mm is taken between the grips. The test specimen was prepared by machining operation.

Tensile strength is obtained from the experimental data using,

$$\begin{aligned} \text{Tensile strength} &= \text{load break/ original cross sectional area} \\ &= L/b \times d \end{aligned}$$

L = Load applied in N, b = width in mm, d = thickness in mm

$$L = \Delta P / \Delta \delta$$

**Flexural properties:** Flexural properties were studied as per ASTM D790 using specimen with a dimension of 3mm in depth, 10mm width and 90mm in length using Instron testing machine at 2mm/min cross head a speed. Flexural strength is the maximum stress developed when a bar shaped test piece acting as a simple beam is subjected to a bending force perpendicular to the bar. It is calculated as follows

$$\text{Flexural strength (s)} = P \times L/bd^2$$

P = Load at a given point with deflection curve, L = Length of the support span, d = width of the bar (mm), b = depth of the beam (mm).

### Impact properties: Fracture Toughness

Fracture test was performed on an (HTE–Series–H50K–S model, Hounsfield test equipments Ltd. UK) hydraulic testing machine at a crosshead speed of 10mm/min according to ASTM D 5045-99. The single edge notch bending (SENB) specimens including notch were cast from the rubber mold, their upper surfaces were machined, and the specimen were pre-cracked by tapping a fresh razor blade frozen in liquid nitrogen in to notch.

### Measurement of flame and water resistance

**Limiting oxygen index (LOI):** LOI test was performed, according to the ASTM D-2863 specification. The relative flammability of the sample bar was determined by measuring the minimum concentration of oxygen, which would just support flaming combustion of the sample bar.

**Water absorption behaviour :** Test specimens prepared as per ASTM D 570 were immersed for 24 hours at 30°C and the percentage of water absorbed by the specimen in calculated using equation given below

$$\% \text{Water absorption} = (w_2 - w_1) \times 100 / w_1$$

Where,  $w_1$  is the initial weight of the sample and  $w_2$  is weight of the sample after immersion in water for 24h at 30°C.

## RESULTS

Spectroscopic analysis

FTIR spectroscopy analysis: The FTIR spectrum of DOPO-epoxy is shown in Fig.1.

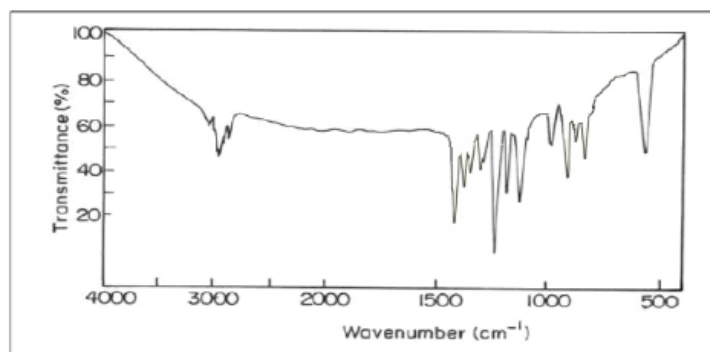


Figure 1: FTIR spectrum of DOPO-epoxy

The FTIR a spectrum of bis (3-aminophenyl) phenyl phosphine oxide (BAPPO) is shown in Fig.2.

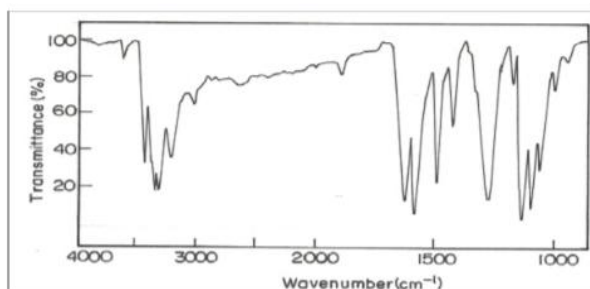


Figure 2: FTIR spectrum of BAPPO

The FT-IR spectrum of phosphorus tetraglycidyl epoxy is shown in Fig.3.

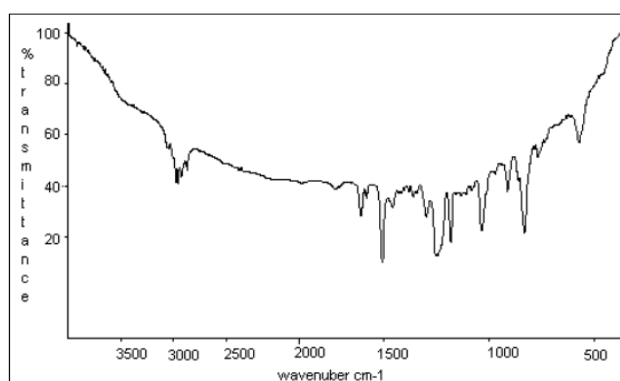


Figure 3: FTIR spectrum of phosphorus tetraglycidyl epoxy

The FTIR spectrum of DDM cured epoxy resin is shown in Fig.4.

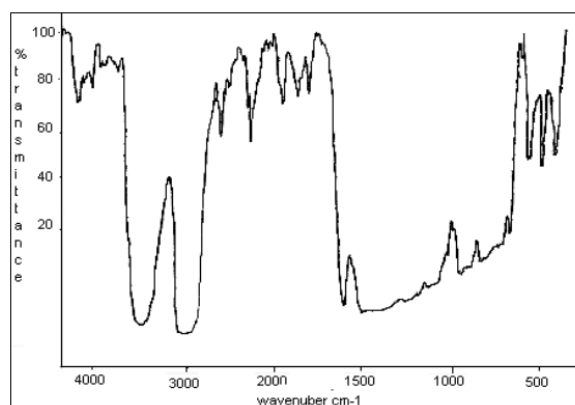


Figure 4: FTIR spectrum of DDM cured epoxy resin

The FTIR spectrum of POSS-NH<sub>2</sub> is depicted in Fig.5.

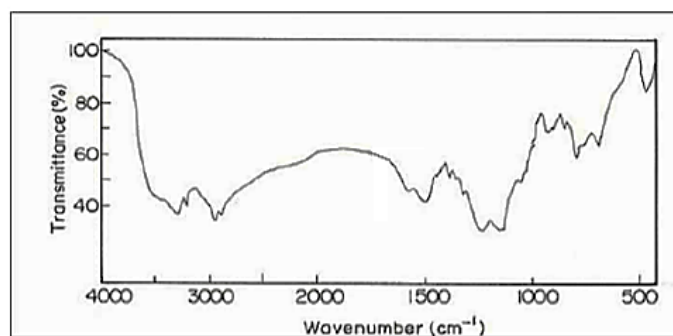


Figure 5: FTIR spectrum of POSS-NH<sub>2</sub>

<sup>1</sup>H NMR spectroscopy analysis

The <sup>1</sup>H NMR spectrum of DOPO-epoxy is shown in Fig.6.

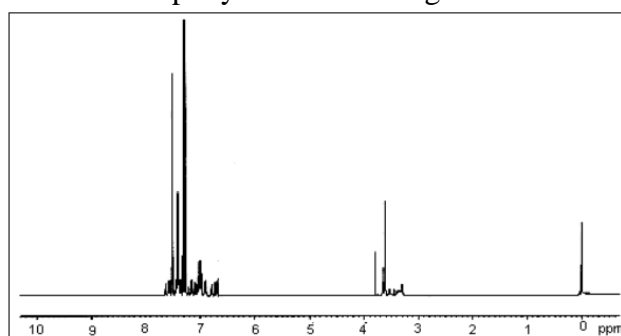


Figure 6: <sup>1</sup>H NMR spectrum of DOPO-epoxy

The  $^1\text{H}$  NMR spectrum of BAPPO is shown in Fig.7.

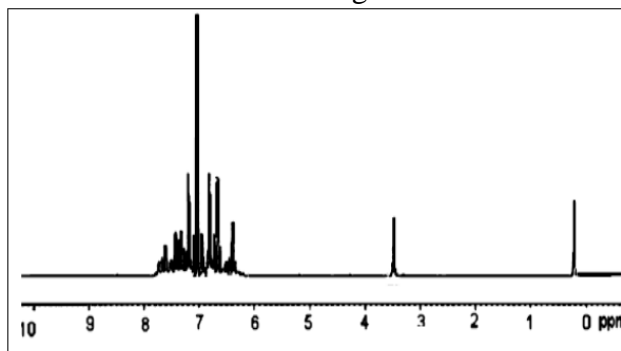


Figure 7:  $^1\text{H}$  NMR spectrum of BAPPO

The  $^1\text{H}$  NMR spectrum of phosphorus tetraglycidyl epoxy is shown in Fig.8.

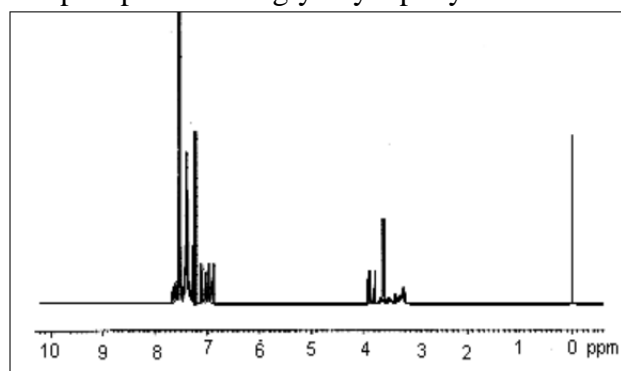


Figure 8:  $^1\text{H}$  NMR spectrum of phosphorus tetraglycidyl epoxy

The  $^1\text{H}$  NMR spectrum of POSS-amine is shown in Fig.9.

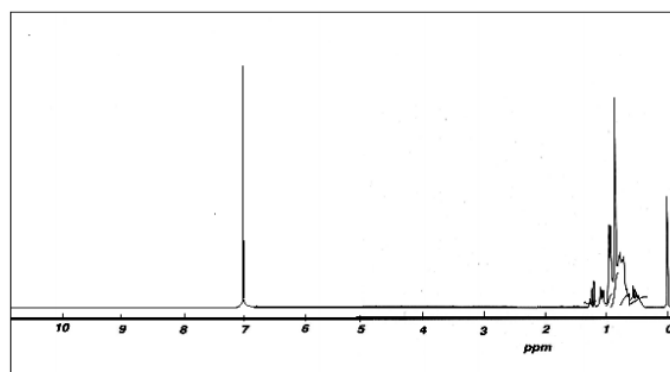


Figure 9:  $^1\text{H}$  NMR spectrum of POSS-amine

The TGA curves of pure DOPO diglycidyl epoxy system and the systems modified with nanoclay are shown in Fig.10.

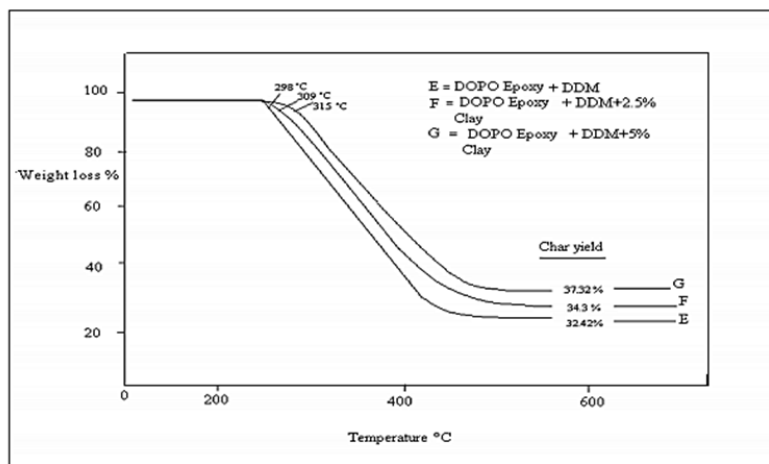


Fig.10. TGA curves of the pure DOPO diglycidyl epoxy system and the systems modified with nanoclay

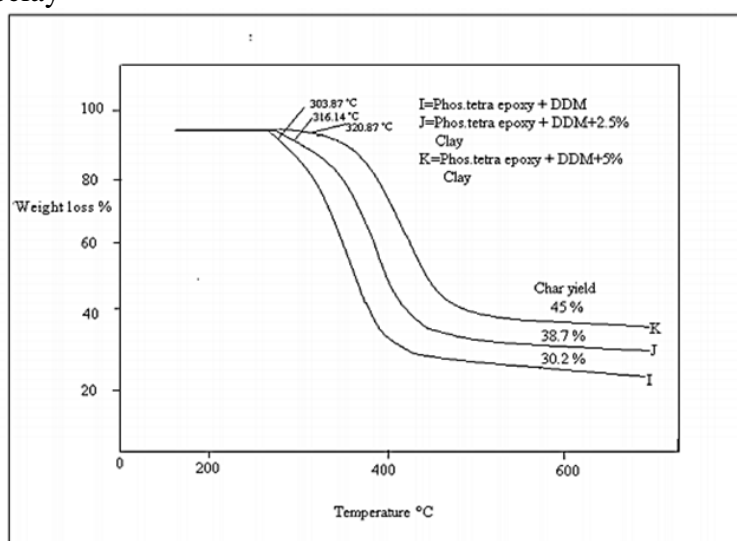


Fig.11. TGA curves of the pure phosphorus tetraglycidyl epoxy system and the systems modified with nanoclay ‘I’, ‘J’, ‘K’

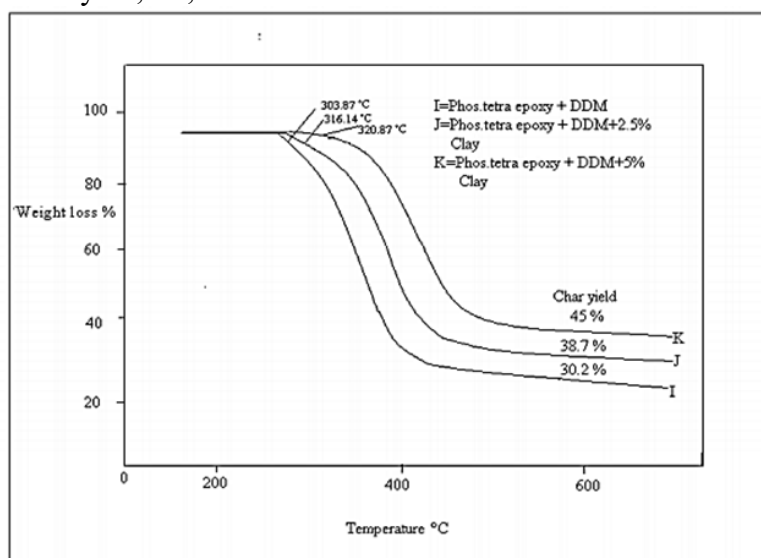


Fig.12. TGA studies of the di and tetraglycidyl phosphorus epoxy systems (‘H’ and ‘L’ respectively) modified with POSS-amine.

## DISCUSSION

### Spectroscopic analysis

#### FTIR spectroscopy analysis

The FTIR spectrum of DOPO-epoxy is shown in Fig.1. The peak at around  $1240\text{ cm}^{-1}$  corresponds to the vibration of the P=O moiety, which is the characteristic of the DOPO molecule. The peaks appear at  $1118\text{ cm}^{-1}$  and  $761\text{ cm}^{-1}$ , are attributed to P-O-C stretching. The absorption peak at about  $3416\text{ cm}^{-1}$  is attributed to the presence of secondary hydroxyl group formed due to epoxy-DOPO reaction. Other IR absorption bands at  $911\text{ cm}^{-1}$  confirm the presence of oxirane ring.

The FTIR a spectrum of bis (3-aminophenyl) phenylphosphine oxide (BAPPO) is shown in Fig.2. The characteristic peaks appear at  $3499\text{ cm}^{-1}$  and  $3393\text{ cm}^{-1}$  confirm the presence Ph-NH<sub>2</sub> group. The absorption band for P-O-Ph stretching appears at  $1093\text{ cm}^{-1}$ . The peak appearing at  $1277\text{ cm}^{-1}$  confirms the presence of P=O group. Other IR absorption band at  $1498\text{ cm}^{-1}$  is attributed to the P-Ph stretching. The FT-IR spectrum of phosphorus tetraglycidyl epoxy is shown in Fig.3. The absorption band at  $909\text{ cm}^{-1}$  is due to the presence of oxirane ring. The aromatic C-C ring stretching occurs at  $1530$  and  $1597\text{ cm}^{-1}$  respectively. The absorption band for C-N stretching of aromatic occurs at  $1351\text{ cm}^{-1}$ . Other IR absorption band at  $2922\text{ cm}^{-1}$  is due to the aromatic C-H stretching.

The FTIR spectrum of DDM cured epoxy resin is shown in Fig.4. The disappearance of oxirane ring at  $906\text{ cm}^{-1}$  and appearance of secondary -OH peak at  $3460\text{ cm}^{-1}$  confirm epoxy-amine curing reaction. The FTIR spectrum of POSS-NH<sub>2</sub> is depicted in Fig.5. The peaks corresponding to -NH<sub>2</sub> and -CH<sub>2</sub> group of POSS-NH<sub>2</sub> appear at  $3500\text{ cm}^{-1}$  and  $2900\text{ cm}^{-1}$  respectively. Furthermore, absorption peaks appeared at  $1200\text{ cm}^{-1}$ - $1300\text{ cm}^{-1}$  and  $1500\text{ cm}^{-1}$  confirmed the presence of Si-O-Si linkage and -Si-CH<sub>2</sub> respectively

#### <sup>1</sup>H NMR spectroscopy analysis

The <sup>1</sup>H NMR spectrum of DOPO-epoxy is shown in Fig.6. The signal at 6.5-7.5 ppm may be due to the aromatic proton. The remaining oxirane and methylene protons adjacent to oxirane appear at 3.2-4.5 ppm.

The <sup>1</sup>H NMR spectrum of Bis (3-aminophenyl) phenylphosphine oxide (BAPPO) is shown in Fig.7. The resonance signal at 3.45ppm confirms the presence of -NH<sub>2</sub> group. The signal at 6.62-7.13 ppm may be due to the aromatic amine proton (C<sub>6</sub>H<sub>4</sub>-NH<sub>2</sub>). The remaining signal appears at 7.4-7.9 ppm may be due to aromatic protons. The <sup>1</sup>H NMR spectrum of phosphorus tetraglycidyl epoxy is shown in Fig.8. The signal at 6.5-7.5 ppm may be due to the aromatic proton. The remaining oxirane and methylene protons adjacent to oxirane appear at 3.2-4.5 ppm. The <sup>1</sup>H NMR spectrum of POSS-amine is shown in Fig.9. The signal at 0.64 ppm may be due to the Si-CH<sub>2</sub> protons. The signal at 1.4 corresponds to C-NH<sub>2</sub> protons.

#### Discussion on thermal stability

##### Thermogravimetric Analysis (TGA)

TGA studies were carried out to examine the effect of incorporation of phosphorus, nanoclay and nano-reinforcement on the thermal stability of both DOPO diglycidyl epoxy resins and phosphorus tetraglycidyl epoxy resins. The incorporation of nano clay into both DOPO

diglycidyl epoxy system and phosphorus tetraglycidyl epoxy system increases the thermal degradation temperature according to its percentage concentration.

The TGA curves of the pure DOPO diglycidyl epoxy system and the systems modified with nanoclay are seen in Fig.10. From the figure it is clearly seen that addition of clay enhances the initial degradation temperature. For example the initial degradation temperature for the pure DOPO diglycidyl epoxy resin (system 'E') is 298°C. The addition of 2.5% clay in the DOPO diglycidyl epoxy (system 'F') increases the initial degradation temperature to 300°C. Further increasing the percentage of nanoclay to 5% (system 'G') the initial degradation temperature is raised to 320°C. This could be attributed to the fact that the presence of clay prevents the evolution of volatile degradation products by acting as a physical barrier [21].

The TGA curves of the pure phosphorus tetraglycidyl epoxy system and the systems modified with nanoclay 'I'; 'J', 'K' are seen in Fig.11. From the figure it is clearly seen that addition of clay enhances the initial degradation temperature, as observed for the DOPO diglycidyl epoxy systems. The TGA studies of the di and tetraglycidyl phosphorus epoxy systems ('H' and 'L' respectively) modified with POSS-amine is shown in Fig.12. From the graphs, similar trend in behaviour is observed for both the DOPO diglycidyl and phosphorus tetraglycidyl epoxy resins. The systems 'H' and 'L' undergo initial degradation at 322°C and 335°C respectively. It is also observed that the incorporation of POSS-amine increases the thermal degradation temperature due to the presence Si-O-Si moiety, which delays the thermal degradation. While heating, the lower surface energy of silicone renders it migrate to the surface of the epoxy resin to form a self-healing layer with resistance to heat and thus slows down the thermal degradation of the epoxy polymer [22].

## Mechanical characteristics

### Tensile and Flexural Strength

The measured tensile and flexural properties of DOPO difunctional epoxy and phosphorus tetra functional epoxy systems are summarized in the Table.3. The data resulted from mechanical studies indicate that the values of tensile and flexural strength of DOPO diglycidyl epoxy and phosphorus tetraglycidyl epoxy reduced significantly with the addition of nanoclay and nanoreinforcement as seen in Table 3. For example the tensile strength and the flexural strength values for the pure DOPO diglycidyl epoxy resin (system 'E') are 39.11 MPa and 120.8 Mpa respectively. The addition of 2.5% clay in the DOPO diglycidyl epoxy (system 'F') reduces the tensile strength to 32.97 MPa and the flexural strength to 73.8 MPa. Further increasing the percentage of nanoclay to 5% (system 'G'), the tensile and flexural strength are still reduced to 27.53 MPa and 61.3 MPa respectively. The significant reduction in the tensile and flexural strength values may be due to the poor dispersion of the nanoclay in the epoxy resin, wide boundary between the particles and the bubbles trapped during the sample preparation. Furthermore, the unhomogenized network density of the sample and the high stress concentration, which could exist at the interface between the nanoclay and the matrix could also contribute to the reduction in the values of the tensile and flexural strength [17].

The addition of POSS-amine to the DOPO diglycidyl epoxy resin (system 'H') also reduces the tensile and flexural strength values to 33.72 MPa and 82.1 MPa respectively. The reduction in the strength of nano-reinforced (POSS-amine) epoxy may be explained due to the weak molecular attraction of pendant groups present in the siloxane molecule as well as weak interface boundary between siloxane molecule and epoxy matrix. However the values of tensile and flexural strength of POSS-nanomer reinforced epoxies systems are slightly

higher than those of the nanoclay reinforced epoxy systems. This is due to the mono functional amine group present in the POSS, which slightly increased the cross-linking density in the systems [18]. Similar behavior is observed for the tetraglycidyl phosphorus epoxy resin systems 'I','J','K'and 'L' which show a higher tensile and flexural strength values owing to their high functionality when compared with DOPO diglycidyl epoxy resins.

### Impact properties -Fracture Toughness

The values of the fracture toughness of DOPO diglycidyl epoxy, phosphorus tetra functional epoxy is summarized in Table 3.

**Table 3. Results of mechanical studies**

Resin system	Tensile strength (MPa)	Flexural strength (MPa)	Fracture toughness (MPa)
E	39.11	120.8	0.72
F	32.97	73.8	0.78
G	27.53	61.3	0.98
H	33.72	82.1	1.45
I	65.4	173.8	0.79
J	37.69	80.4	0.86
K	31.23	69.6	1.02
L	38.28	95.8	1.62

The data indicate that the fracture toughness increased significantly with the addition of nanoclay and nanoreinforcement. For example the fracture toughness values for the pure DOPO diglycidyl epoxy resin (system 'E') is 0.72 Mpa. The addition of 2.5% clay in the DOPO diglycidyl epoxy (system 'F') increases the fracture toughness value to 0.78 Mpa. Further increasing the percentage of nanoclay to 5% (system 'G'), the fracture toughness values is found to be increased to 0.98 Mpa. The reason for the increase in impact strength may be that the clay particles would act as crack stoppers and forms a tortuous crack propagation path resulting in higher impact strength [19].The addition of POSS-amine to the DOPO diglycidyl epoxy resin (system 'H') also increases the fracture toughness values to 1.45 Mpa. This may be explained by the pinning effect, which prevents crack opening [20]. Similar kind of behaviour is exhibited by the phosphorus tetraglycidyl systems 'I','J','K' and 'L' but they exhibit higher values of fracture toughness than the DOPO diglycidyl epoxy systems.

### Flame and water resistance

#### Limiting Oxygen Index (LOI): Flame retardant studies

The LOI is defined as the minimum fraction of oxygen from oxygen nitrogen mixture, which is sufficient to sustain combustion of the specimens after ignition. The LOI value can be used as an indicator to evaluate the flame retardancy of polymers. Most phosphorus containing epoxy polymers possess high char yields. It has been reported that higher char yields and larger LOI values are indicative of better flame-retardant properties [25]. LOI and char residue values for all of the epoxy systems are shown in Table 4. It is seen that the LOI and char residue is higher for the systems containing clay and POSS-amine.

In the case of the systems containing clay, the system'G' containing 5% clay is found to exhibit better LOI and char yield, i.e. 34.37 and. 37.32 respectively, which is higher than the

system 'F' containing 2.5% clay which exhibits a LOI and char yield of 33.24 and 34.3 respectively. Similar trend is shown by the tetraglycidyl phosphorus epoxy systems 'J' and 'K' modified with clay. The char forming nature of clay is the main reason for its better LOI and char yield. [26]

**Table.4. Flame retardancy studies of epoxy systems**

Resin System	LOI	Char residue
E	32.42	32.42
F	33.24	34.3
G	34.37	37.32
H	35.87	36.6
I	29.48	30.2
J	32.88	38.7
K	35.4	45.0
L	38.6	38.0

As seen in the Table 4 the DOPO diglycidyl epoxy and tetraglycidyl phosphorus epoxy systems on the addition of poss-amine ('H' and 'L' respectively) exhibited the maximum LOI and char yield of 35.87, 36.6 and 38.6, 38.0 respectively. This could be due to the synergistic char protecting effect of both siloxane and phosphorus moiety present in the DOPO diglycidyl epoxy and tetraglycidyl phosphorus epoxy systems which has been modified with POSS-amine. [27-28].

### Water Absorbance

The water resistant behaviors of various systems are tabulated in Table 5. The water absorption tendency is found to decrease on addition of both clay [29] and POSS-amine [30], which is due to the hydrophobic and partial ionic nature of Si-O-Si linkage. In the case of the systems containing clay, the system 'G' containing 5% clay is found to exhibit better water resistant behavior, i.e. 0.021% water absorbance than the system 'F' containing 2.5% clay which shows 0.027% water absorbance. Similar trend is shown by the tetraglycidyl phosphorus epoxy systems 'J' and 'K' modified with clay.

**Table.5. Water absorbance of epoxy systems**

Resin System	% of Water absorbance
E	0.082
F	0.027
G	0.021
H	0.012
I	0.034
J	0.025
K	0.012
L	0.010

The diglycidyl and tetraglycidyl phosphorus epoxy resin systems 'H' and 'L' modified with POSS-amine show the least i.e. 0.12% and 0.10% water absorbance. This might be attributed to the inherent hydrophobic nature imparted by the Si-O-Si linkage present in the nanoreinforcement [31-32].

## CONCLUSIONS

In the present work a comparative study has been done on phosphorus containing di and tetraglycidyl epoxy resin systems. The diglycidyl epoxy chosen was DOPO epoxy. It was synthesized by reacting DOPO with DGEBA. The phosphorus tetraglycidyl epoxy chosen was synthesized from BAPPO using a reported procedure. The di and tetra glycidyl epoxies synthesized were characterized by IR and  $^1\text{H}$  NMR spectroscopic methods. Nanoclay and POSS-amine were incorporated into the epoxy resins and a comparative study on the mechanical, thermal, flame retardant, water absorption characteristics of two types of epoxies was done. It was observed that the incorporation of nanoclay and nano-reinforcement into the epoxy systems decreased the tensile and flexural properties due to the plasticizing effect of nanoclay and the flexible Si-O-Si linkage in the nanoreinforcement but the fracture toughness was found to be increased, this could be attributed to the fact that nanoclay functioned as crack stoppers and formed a tortuous crack propagation path that resulted in higher impact strength and due to the pinning effect, which prevented crack opening in the case of the nanoreinforcement. The thermal properties of both the di and tetraglycidyl resins were found to increase on the addition of nanoclay and nano-reinforcement, which could be due to the barrier properties of nanoclay and self-healing property of nano-reinforcement. The flame retardant behaviour of these resins showed that the system containing nano-reinforcement showed high LOI, this could be due to the synergistic effect of siloxane and phosphorus. The water absorption behaviour of the resins was studied and it was found that the epoxy resin systems containing nano-reinforcement showed the best results due to the hydrophobic behaviour of Si-O bonds. In all the studies undertaken, the phosphorus tetraglycidyl epoxy resin system modified with nano-reinforcement showed the best results over the phosphorus modified diglycidyl epoxy resin systems, emphasizing their suitability in high performance aerospace applications.

## ACKNOWLEDGEMENTS

The authors are grateful to Department of Science and Technology for having provided financial assistance to carry out this work and thankful to Anna University, Chennai, India for providing necessary facilities for this work.

## REFERENCES

1. Cheng, K.C, Lai K.C, Chiu W.J. (1999) Journal of Applied Polymer Science, 71, 721-28.
2. May, C.A (Ed.) (1988) Epoxy resins-chemistry and technology 2nd Ed. New York: Marcel Dekker.
3. Lee H and Nevellie K. (Eds.) (1967) Handbook of epoxy resin, New York: McGraw-hill.
4. Wong, C.P. (1988) Advances in Polymer Science, 84,63-83.
5. Cheng K.C. (1998), Journal of Polymer Science –Part. B Polymer Physics 36, 2339-45.

6. Buckingham M.R., Lindsay A.J., Stevenson D.E., Muller G, Morel E, Costes B, Henry Y(1996) *Polymer Degradation and Stability* 54, 311-15.
7. Cheng kuo-chung, Yu Su-yun, Chiu wenyen (2002) *Journal of Applied Polymer Science* 83, 2741-56.
8. Ananda kumar S, Denchev Z and Alagar M. (2006) *European Polymer Journal* ,42,2419-29
9. Wang C.S and Sheigh J.Y. (1998) *Polymer*.39,5819-26.
10. Hussain M and Simon G.P. (2003) *Journal of Material Science Letters* 22, 1471- 75.
11. Kornmann X, Lindberg H, Berglund L.A.(2001) *Polymer*. 42, 1303-10.
12. Woo R.S.C, Chen Y.H, Zhu H.G, Leung C.K.Y, Kim J.K. (2008) *Composite Science and Technology* 68, 2149-55.
13. Plinio Innocenzio and Tongjit Kidchob (2005) *Journal of Sol-Gel Science Technology*, 35, 225-35.
14. Jiwon Choi, Jason Harcup, Albert F.Yee, Quan Zhu, Laine RM. (2001) *Journal of American Chemical Society* 123,11420-24.
15. Guizhi Li, Lichang Wang, Hanli Ni, Charles U. Pittman Jr.(2002) *Journal of Inorganic and Organomettalic Polymers* , 11, 123-54.
16. Tae-Ho Lee, Jeong Hwan Kim and Byeong-Soo Bae (2006) *Journal of Materials Chemistry*, 16, 1657-64.
17. Chen J.S, Poliks M.D, Ober C.K, Zhang Y, Giannelis E.(2002) *Polymer*, 43, 4895-904.
18. Qi B, Zhang QX, Bannister M, Mai YW. (2006) *Composite Structure*, 75, 514-19.
19. Ghader Khanbabaei, Jamal Aalaie, Ali Rahmatpour, Alireza Khoshniyat (2007) *Journal of Macromolecular Science B: Physics*, 46, 975-86.
20. Jones I.K, ZhouY.X, Jeelani S, Mabry J.M.(2008) *eXPRESS Polym Lett*, 2, 494-501.
21. Wang H, Hoa SV, Wood-Adams PM.(2006) *Journal of Applied Polymer Science*, 100, 4286-96.
22. Camino G, Tartaglione G, Frache A, Manferti C, Costa G (2005) *Polymer Degradation and Stability* 90, 354-62.
23. Liu G.H, Hsiue, Lan C.W and Chiu Y.S. (1997) *Polymer Degradation and Stability* 56, 291-99.
24. Ole Beckere. (2001) *Journal of Polymer Science*, 43, 4365-73.
25. Hongzhi Liu, Sixun Zheng and Kangming Nie. (2009) *Macromolecules* 38,5088-93.
26. Kornmann. X, Lindberg H, and Berglund LA(2001) *Polymer*, 42, 1303-10.
27. Becker O, Varley R, Simon G (2002) *Polymer*, 43, 4365-73.
28. Annakutty K.S, and Kishore K. (1988) *Polymer*, 29,1273-76.
29. Liu Y.L, Hsiue G.H, Lan C.W, Chiu Y.S.(1997) *Polymer Degradation and Stability* 56,291-99.
30. Liu W.P, Hoa S.V, Pugh M.(2005) *Composites Science and Technology*, 65,2364-72.
31. Haque A, Shamsuzzoha M., Hussain F, Dean D.J.(2003) *Composite Materials* 37,1821-37.
32. Zhang C.J, Laine R.(1999) *Organomettalic Chemistry* 521, 199-201.